Field Crops Research 221 (2018) 98–107

Contents lists available at ScienceDirect

Field Crops Research

journal homepage: www.elsevier.com/locate/fcr

# Assessing yield and fertilizer response in heterogeneous smallholder fields with UAVs and satellites

Antonius G.T. Schut[a,*], Pierre C. Sibiry Traore[b,c], Xavier Blaes[d], Rolf A. de By[e]

[a] Plant Production Systems Group, Department of Plant Sciences, Wageningen University and Research Centre, Wageningen, The Netherlands
[b] MANOBI, Fenetre Mermoz V17, POB 25026, Dakar-Fann, Senegal
[c] International Crops Research Institute for the Semi-Arid Tropics (ICRISAT), Samanko Stn., POB 320, Bamako, Mali
[d] Earth and Life Institute, Université Catholique de Louvain, Croix du Sud L5.07.16, B-1348 Louvain-la-Neuve, Belgium
[e] Department of Geo-Information Processing, Faculty of Geo-information Science and Earth Observation, University of Twente, The Netherlands

ARTICLE INFO

*Keywords:*
UAV
Agriculture
Ground coverage
Spatial variability
Smallholder landscapes

ABSTRACT

Agricultural intensification and efficient use and targeting of fertilizer inputs on smallholder farms is key to sustainably improve food security. The objective of this paper is to demonstrate how high-resolution satellite and unmanned aerial vehicle (UAV) images can be used to assess the spatial variability of yield, and yield response to fertilizer. The study included 48 and 50 smallholder fields monitored during the 2014 and 2015 cropping seasons south-east of Koutiala (Mali), cropped with the five major crops grown in the area (cotton, maize, sorghum, millet and peanuts). Each field included up to five plots with different fertilizer applications and one plot with farmer practice. Fortnightly, in-situ in each field data were collected synchronous with UAV imaging using a Canon S110 NIR camera. A concurrent series of very high-resolution satellite images was procured and these images were used to mask out trees. For each plot, we calculated vegetation index means, medians and coefficients of variation. Cross-validated general linear models were used to assess the predictability of relative differences in crop yield and yield response to fertilizer, explicitly accounting for the effects of fertility treatments, between-field and within-field variabilities. Differences between fields accounted for a much larger component of variation than differences between fertilization treatments.

Vegetation indices from UAV images strongly related to ground cover ($R^2 = 0.85$), light interception ($R^2 = 0.79$) and vegetation indices derived from satellite images ($R^2$ values of about 0.8). Within-plot distributions of UAV-derived vegetation index values were negatively skewed, and within-plot variability of vegetation index values was negatively correlated with yield. Plots on shallow soils with poor growing conditions showed the largest within-plot variability. GLM models including UAV derived estimates of light interception explained up to 78% of the variation in crop yield and 74% of the variation in fertilizer response within a single field. These numbers dropped to about 45% of the variation in yield and about 48% of the variation in fertilizer response when lumping all fields of a given crop, with $Q^2$ values of respectively 22 and 40% respectively when tested with a leave-field-out procedure. This indicates that remotely sensed imagery doesn't fully capture the influence of crop stress and management. Assessment of crop fertilizer responses with vegetation indices therefore needs a reference under similar management. Spatial variability in UAV-derived vegetation index values at the plot scale was significantly related to differences in yields and fertilizer responses. The strong relationships between light interception and ground cover indicate that combining vertical photographs or high-resolution remotely sensed vegetation indices with crop growth models allows to explicitly account for the spatial variability and will improve the accuracy of yield and crop production assessments, especially in heterogeneous smallholder conditions.

## 1. Introduction

Yields in smallholder fields are often only 20% of attainable yields (Tittonell and Giller, 2013). Yield gaps are usually defined as the difference between water-limited and actual yields (van Ittersum et al., 2013). These yield gaps may be caused by many factors, including management (choice of crop variety, suboptimal plant density and sowing dates, limited use of fertilizers, weeding, pest and disease

* Corresponding author.
*E-mail addresses:* tom.schut@wur.nl (A.G.T. Schut), pierre.sibiry.traore@manobi.com (P.C.S. Traore), xavier.blaes@uclouvain.be (X. Blaes), r.a.deby@utwente.nl (R.A. de By).

https://doi.org/10.1016/j.fcr.2018.02.018
Received 23 June 2017; Received in revised form 15 February 2018; Accepted 18 February 2018

control) and biophysical constraints (pH, macro- and micro nutrient availability). There is an urgent need to sustainably intensify to feed the fast growing populations in sub-Saharan Africa, while limiting expansion of agricultural land-use (van Ittersum et al., 2016). Reliable estimates of attainable yields and realized production at field and farm scales are needed to better inform policy makers, farmers and suppliers of inputs and credit, to more effectively intensify and ensure that inputs are targeted efficiently. Farmer investments in intensification are driven by the expected return on investment, for which reliable knowledge about the expected yield response (the additional kg of yield per kg of nutrient applied) is key information but known to vary strongly over small distances, governed mostly by influence of past management (Zingore et al., 2011). Better information about the differences in the response to applied nutrients within and between fields may help maximize financial returns for smallholders and other investors.

Quantitative information about crop management and crop growth may help inform government agencies and actors in agricultural value chains. This will help to accelerate the intensification of smallholder farming systems by improving credit facilities, input supply mechanisms and market options. Smallholder farming systems in sub-Saharan Africa are highly diverse. Spatial variability is large intra-field, as trees are omnipresent in fields and inter cropping or relay cropping (e.g. peanuts and watermelon) is common. Environmental conditions (soil type, fertility and water availability) vary strongly within landscapes and even within fields (Tittonell et al., 2008). Natural spatial variability is further compounded by heterogeneous management practices (Tittonell et al., 2005a). Socio-economic factors also play an important role as nutrient re-distribution by grazing animals and use of crop residues cause strong gradients in soil fertility, typically decreasing with distance to the homestead (Tittonell et al., 2005b).

Precise monitoring of crop growth in smallholder fields with abundant trees requires a time-series of very high resolution (VHR) images, as observed spatial patterns in vegetation indices over cropland areas change through time due to interactions between site, weather and management. Interpreting these spatial patterns is therefore not straightforward. For example, spatial patterns in the landscape may emerge during the season due to staggered planting practices and differences between crops in phenology, such as greening up rate and plant senescence (Schut et al., 2010). Interpreting such spatial patterns in smallholder landscapes in terms of yield or nutrient response is therefore not straightforward, especially if only one single image is available as sowing windows are typically wide, with frequent re-sowing or transplanting when needed. A time-series of images may resolve these temporal aspects in the observed spatial patterns, and may be much more useful to assess differences in yield than one in-season image. Further, a very high-resolution dry season-image provides means to map evergreen tree locations, needed to eliminate the influence of trees on signals from the crop. Available optical satellite products are limited in that regard by their temporal resolution and their cost (e.g. DigitalGlobe, Pleiades), by their spatial resolution (e.g. MODIS, SPOT-Vegetation, Proba-V), and by cloud cover during the growing season (all).

Unmanned Aerial Vehicle (UAV) systems do not suffer from such strong cloud cover limitations and may present a useful alternative to monitor crop growth. Also, they can be used to upscale plot data collected at a limited number of locations to wider areas (van der Heijden et al., 2007), providing means to upscale plot-based assessments at relatively low costs. Unmanned aerial vehicles have been widely used experimentally to monitor crops, e.g., for assessment of plant survival and necrosis (Khot et al., 2016), precision agriculture (Zhang and Kovacs, 2012), and plant phenotyping (Sankaran et al., 2015). With UAV high-resolution images, crop height can be derived from surface models (Bendig et al., 2014), and strong relationships with biomass have been reported (Li et al., 2016). Most uses of UAV images are in the context of high-input farming systems. To our knowledge, there is no example of UAVs used to assess crop yield and its response to nutrients in smallholder landscapes (Burke and Lobell, 2017).

In previous work, we showed that only about 50% of the within-field variation in vegetation index values can be explained by fertilization treatments (Blaes et al., 2016). We further showed that on a landscape scale, the fraction in normalized difference vegetation index (NDVI) variability attributable to fertilization treatment (1–23%) was much smaller than the fraction attributable to between-field differences arising from soil variability or other field management practices. Fields within the same soil catena position were shown to be more alike, indicating that catena and the interaction with farm management strongly affect vegetation index values. Vegetation indices most strongly respond to ground cover, while both ground cover and vegetation indices correlate with light interception by the crop. Interception of photosynthetically active radiation is causally related to the crop growth rate (Sinclair and Muchow, 1999) and accumulated crop growth rates during grain filling determine crop yield (Goudriaan and Van Laar, 1994).

Combining vegetation indices from image time-series with crop growth models may provide means to develop a better understanding of underlying processes (Bouman and Goudriaan, 1989). Images may also inform about field conditions and crop status, e.g. spatial variability at small scales may inform about plant density variations. We aim to improve quantitative information on smallholder crop growth that enable better links between crop growth models and actual farmer yields using UAV and satellite data. The objective of this work is to test whether UAV images can be used to assess differences in light interception and crop yields between smallholder fields, and responses to fertilizer therein. The latter may be interpreted as an approximation of the nutrient gap, i.e. the extra yield that can be obtained when comparing to an adequate fertilization reference. Secondly, we expect that small-scale spatial variation may be an indicator of plant heterogeneity and a proxy for poor crop growth conditions. We hypothesize that knowledge of light interception and coefficients of spatial variation helps to assess and explain differences in crop yield and response to fertilizer between fields.

## 2. Materials and methods

### 2.1. Field data

During the 2014 and 2015 growing seasons, we collected ground data in respectively 48 and 50 farm fields near Sukumba (Koutiala District, Mali). The Sukumba village is located in the Sudano-Sahelian climate zone, with an average annual rainfall of about 900 mm (Traore et al., 2013). Crops monitored included Maize, Peanut, Sorghum, Millet and Cotton. Fields were located along a catena, covering light colored alluvial valley soils with deep sandy loams (subsoil: clay loams), shallow red colored sandy loams with gravelly material on intermediate landscape positions and again somewhat deeper soils with sandy loam topsoils and higher sub-surface clay contents, on plateau positions. Fields were thus grouped into three broad strata (valley, intermediate and plateau) based on combinations of soil type and elevation. Soil types were derived from a map used for a regional study (PIRT-Projet Inventaire des Ressources Terrestres, 1983). Each field included five or six plots of 225 $m^2$ (15 × 15 m) with different crop-specific fertilizer application rates. Plot A reflected farmer practice, plot B did not receive fertilizer and plots C to F received increasing amounts of fertilizer. These plots were located at least 5 m away from the crown of trees, ensuring that trees did not influence crop growth or UAV images. On average, fields were sown around June 2nd (millet), June 5th (cotton) and June 19th (maize, peanut and sorghum). Crops were mostly manually sown, leading to wide sowing windows with standard deviations around these mean sowing dates of 16.4, 9.6, 7.9, 9.2 and 21.7 days for millet, cotton, maize, peanut and sorghum, respectively in 2014. Harvest dates varied a bit more: peanut was harvested first around October 3rd (± 5.2 days), followed by cotton (November

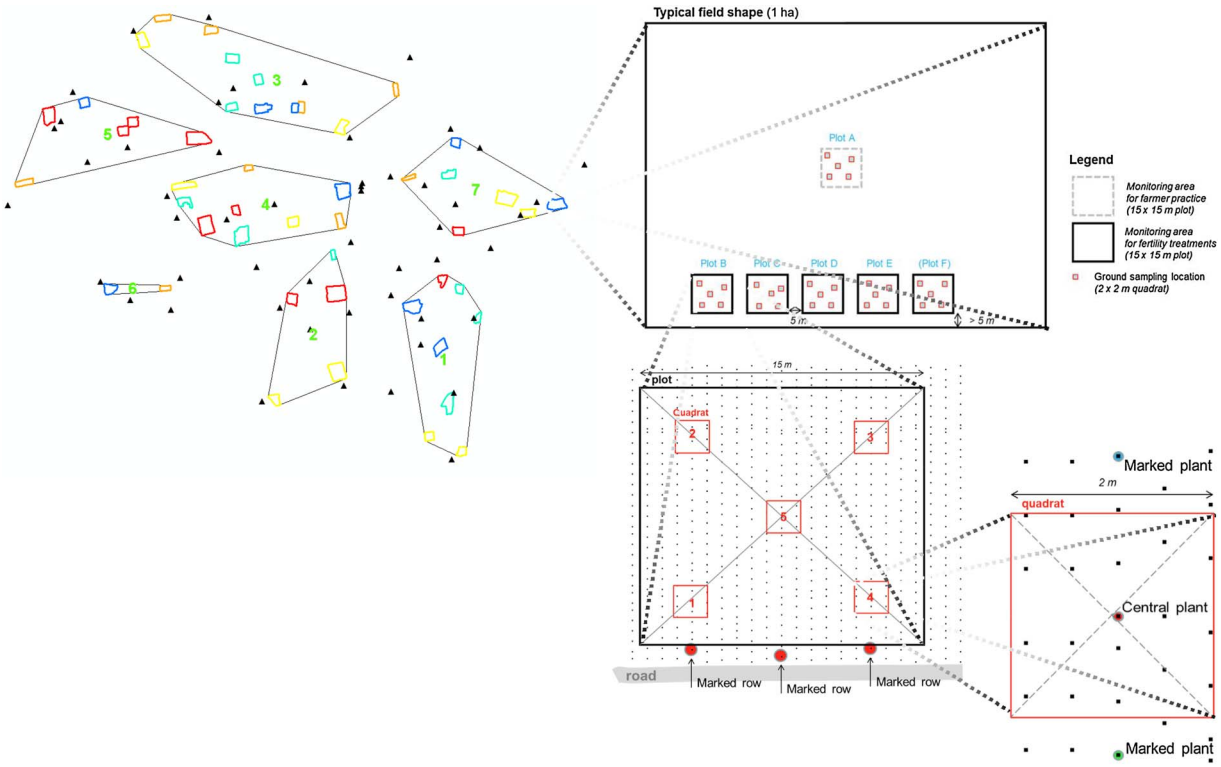


**Fig. 1.** The 2014 experimental layout for UAV and ground monitoring of 48 farmer fields (colored outlines), each including up to six fertility treatment plots of 225 $m^2$ each, within which five quadrats of 4 $m^2$ were used for ground data collection. The 48 fields were organized in seven flight clusters (black outlines), each including ground control points (black triangles). The colors for the field boundaries reflect crop type (yellow for cotton, cyan for millet, blue for sorghum, red for maize and orange for peanut). The 2015 layout was similar with 50 fields monitored from the same flight area (with about half reconducted from 2014 owing to crop rotations). (For interpretation of the references to colour in this figure legend, the reader is referred to the web version of this article.)

1st ± 5.2), maize (November 7th ± 17.2), sorghum (November 17th ± 5.6) and millet (November 29th ± 7.3).

From the second week of August 2014 onwards, data was collected fortnightly in the field in five 4 $m^2$ quadrats. One quadrat was placed in the center of the plot, the other four quadrats were placed on each plot diagonal at 1/3 of the distance from the plot corners towards the center (Fig. 1). In each quadrat, we measured the height of five individual plants with a ruler and we assessed ground coverage with a downward facing, vertical photograph using a 3 m telescopic pole. These digital images were processed with CAN-EYE freeware (www6.paca.inra.fr/can-eye) and ground cover (GC) was estimated as the fraction of pixels that was classified as green material (Blaes et al., 2016). Classification in CAN-EYE relies on visual assessment of thresholds, these were determined for each image separately. Ground cover for millet and sorghum were only measured until flowering when crops grew beyond the 3 m pole. At the end of the growing season, all quadrats were harvested. At harvest, fresh matter weights were recorded with a field scale for both reproductive (yield) and vegetative (stover and/or residues) parts. Further details about the data collection protocol can be found elsewhere (Blaes et al., 2015; Blaes et al., 2016).

In 2015, these fortnightly field-based observations and UAV flights were continued during the full growing season, on the same crops but in different fields within the landscape. Blaes et al. (2015) provide a more complete description of experimental details.

### 2.2. UAV data

The SenseFly eBee UAV in use carried a Canon S110 NIR camera with green, red and near-infrared filters. The camera system limitations included spectral overlap in the red and green bands and wide pass-bands (up to about 0.1 µm at half maximum). Channel 2 featured a better visual contrast than channel 1. This section describes how eBee image data was acquired, mosaicked and processed to correct for variations in illumination resulting in pseudo-reflectance values that were used to derive vegetation index values.

The eBee was flown over seven field clusters, including experimental fields and plots (Fig. 1). Each cluster was revisited every fortnight, although exact dates varied due to weather and other operational conditions. The eBee was flown between 10 and 12 a.m. at 286 m above the ground surface, resulting in about 10 × 10 cm pixel sizes. The exploitable spatial resolution however, is coarser due to pervasive image blur, noise and sensor limitations. Image acquisition settings ensured 70% lateral and 75% longitudinal overlap (Blaes et al., 2016).

Generation and mosaicking of ortho-images involved the use of a network of 52 accurately geo-referenced ground control points, production of digital surface models (DSM) for each flight, and correction for variations in illumination conditions with a sensor-specific perpendicular vegetation index, the eBeePVI, following the soil line approach (Rondeaux et al., 1996; Xu and Guo, 2013). Full details on UAV processing steps are provided as supplementary material. In the analysis here, only eBeePVI and the difference DSM (dDSM, the difference between pre-and in-season DSM value) was used.

### 2.3. eBeePVI versus light interception and ground coverage

Relationships between eBeePVI, ground cover and measured light interception were determined in an experiment at the ICRISAT research station in Bamako in 2015. The experiment included plots with cotton, sorghum, millet, maize and peanut. Every week, digital pictures were taken from above the canopy and light interception was measured weekly with an AccuPAR instrument (Decagon Devices, USA). Ground coverage was determined from the digital pictures using the protocols as described above. The eBee was also flown over these plots and median plot eBeePVI was determined. From these measurements,

relationships between measured ground coverage, light interception and eBeePVI were determined.

### 2.4. Satellite images

For comparison purposes, cloud-free WorldView-2, GeoEye-1 and Quickbird images acquired on 22 and 30 May, 26 June, 29 July, 26 August, 25 September, 4 and 18 October and on 1 and 14 November in 2014 were orthorectified and atmospherically corrected using STARS processing procedures (Stratoulias et al., 2015), and aligned to the first image of the growing season with Erdas Autosync using a 2nd order polynomial. From these corrected satellite images, median NDVI and PVI values per plot were determined.

UAV-satellite image pairs were selected only when 6 days apart or less, to limit the confounding influences of crop growth and, more importantly, field management between the two dates. For example, weeding practices may cause field greenness to change rapidly in time and space.

### 2.5. Statistical analysis

For each UAV flight, per-plot vegetation index distributions, means, standard deviations, skewness, kurtosis, coefficients of variation and median values were determined. Observed distributions of *eBee*PVI and estimated light interception values were tested for normality ($p < 0.05$) using the one-sample Kolmogorov-Smirnov test. Temporal means were computed over the period from 1 July (2015) or 1 September (2014) to 31 October (or date of harvest, whichever occurred first) for each image-derived variable (median eBeePVI, satellite NDVI, spatial CV values and light interception estimates).

Linear regression models were used to test whether estimates of light interception in combination with coefficients of variation of vegetation indices can: 1) predict relative differences between fields within one crop type; 2) assess crop response to fertilizer; and 3) assess the importance of seasons. Additionally, we tested whether if the difference DSMs (dDSM, indicator of crop height) contained additional information.

To account for yield differences between crop types, plot reproductive material (Y, or kg fresh yield/ha) was divided by the mean Y over all plots (p) in all fields (f) with the same crop type (ct), resulting in relative Y values (RY). These RY values were used to determine the RY response (RYR).

$$RY_{ct,f,p} = \frac{Y_{ct,f,p}}{\overline{Y_{ct}}}$$

The difference between the RY and RV of the fertilizer treatment plot p, and the relative yield of unfertilized plot “B” in the same field provided the relative yield response.

$$RYR_{ct,f,p} = RY_{ct,f,p} - RY_{ct,f,p=B} = \frac{Y_{ct,f,p} - Y_{ct,f,p=B}}{\overline{Y_{ct}}}$$

The same was done for fresh vegetative (V) material, (providing RV and RVR), and the natural logarithm of both GC and eBeePVI-derived light interception estimates.

The B plots received either zero fertilizer (2015 and some fields in 2014) or the same as the farmer practice (plots A) due to late instalment of trials in 2014. This is expected to have little effect as most farmers apply only a limited amount of fertilizer and only for cotton and maize. Further, absolute differences in plot averages between the B plot and plots C, D, E and F were determined for UAV derived eBeePVI and light interception.

In total, six general linear models (GLM) were used to estimate the fraction of variation that can be explained by crop type, catena position, temporal means of light interception and the coefficient of variation of vegetation index values within plots, and interactions among them. Combined data from 2014 and 2015 were used and are presented here, results of a per year analysis are presented in the supplementary materials. Each of these models was used to explain variation in RY, RV, RYR and RVR and included a year factor to account for year-to-year differences. Explanatory variables used for models to explain RYR and RVR variation only included the above-mentioned difference with B-plot values.

The first GLM model (model I) used destructive plant measurements to assess the total amount of variation in yield that was explained by field (farmer management and crop type), and plot (fertilization) effects. The second GLM model (model II) evaluated how accurate differences within a field could be assessed using vertical photographs. The factor plot in model I was therefore replaced by the negative logarithm of ground cover derived from vertical photographs taken in each quadrat on every field visit. The third GLM model (model III) evaluated how differences within a field could be assessed with UAV imagery. Here, explanatory variables derived from eBee images (temporal means of light interception, and coefficient of variation) substituted the plot term in Model 1 to assess the error, and the amount of variation left unexplained. The fourth GLM model (model IV) assessed how much of the between- and within-field variation could be explained using crop type, catena position, mean light interception and the coefficient of variation of vegetation index values within plots and interactions as explanatory variables. The field term was not included, in contrast to models I, II and III. The fifth GLM model (model V) included only estimates of light interception and the spatial coefficient of variation, derived from the distribution of eBeePVI values within one plot. Vegetation indices respond to ground cover, but are also sensitive to chlorophyll contents, leaf stacking and leaf angle distributions. This model provides an estimate of the loss of information when only light interception estimates are used. The sixth GLM model (model VI) was included to analyse the influence of dDSM. It followed the same structure as model V but included year and crop interactions as an extra explanatory factor and dDSM as variable.

Components of variation were assessed using an analysis of variance. Leave-three-random-plots-out and leave-field-out cross-validations were used to test robustness of the regression models. When a field was excluded, it means that all plots on that field were excluded from calibration, similar to using the calibrated model for predictions of relative yield and the response to applied fertilizer for an independent field.

## 3. Results

### 3.1. Observed yields and biomass in the on-farm experiments

The observed average dry matter yields and total biomass amounts are higher in 2014 than in 2015 for cotton, maize and sorghum, whereas peanut yields were higher in 2015 (Table 1). The average yield response to the fertilizer treatments was small, but spatial variability in both yields and yield responses was large with CV values of 0.36–0.66 (Table 1) and standard deviations of yield responses frequently exceeding the means (Table S1, supplementary material), which reflects the wide range of responses that were observed in the experimental fields.

### 3.2. Estimates of light interception

The strong and negative exponential relationship between ground cover (*GC*) and light interception (*LI*) explains 86% of the variation (Fig. 2). The light extinction coefficient for an additional percentage of ground cover is 0.0231. The *eBeePVI* is strongly related to ground cover with an $R^2$ value of 0.85. In principle, when *eBeePVI* is zero, ground cover should also be zero. However, the intercept of the relationship is negative, indicating that some soil pixels can also be found between 0 and 0.053, where the line intersects the *x*-axis. Therefore, an additional term was included in the relationship between *eBeePVI* and light

**Table 1**
Means of yield and total biomass per treatment. The CV values reflect spatial variability in dry matter yield between fields, values were computed as standard deviations of yields recorded per plot, divided by the mean of all plots with the same treatment. Dry matter contents are also provided for grain/beans and for other plant components.

| Plot | Cotton | | Maize | | Peanut | | Millet | | Sorghum | |
|---|---|---|---|---|---|---|---|---|---|---|
| | 2014 | 2015 | 2014 | 2015 | 2014 | 2015 | 2014 | 2015 | 2014 | 2015 |
| | Yield, kg DM ha$^{-1}$ | | | | | | | | | |
| A | 1542 | 1017 | 3737 | 3179 | 1079 | 1204 | 1342 | 1388 | 852 | 1008 |
| B | 1163 | 792 | 4639 | 2664 | 890 | 1560 | 1348 | 1042 | 1131 | 1111 |
| C | 1162 | 1172 | 5213 | 3191 | 1135 | 1523 | 1290 | 1494 | 1205 | 1242 |
| D | 1502 | 1093 | 4939 | 3536 | 1037 | 1520 | 1573 | 1672 | 1697 | 1510 |
| E | 1631 | 1175 | 5711 | 3586 | 1129 | 1492 | 1954 | 1960 | 1999 | 1526 |
| F | | | | | | | 1961 | 1603 | 1795 | 1504 |
| CV | 0.48 | 0.50 | 0.36 | 0.58 | 0.41 | 0.44 | 0.66 | 0.47 | 0.50 | 0.51 |
| DMc grain | 0.93 | 0.92 | 0.86 | 0.74 | 0.61 | 0.60 | 0.92 | 0.80 | 0.90 | 0.80 |
| | Biomass, kg DM ha$^{-1}$ | | | | | | | | | |
| A | 3845 | 2462 | 6930 | 6310 | – | 1682 | 5427 | 4219 | 2747 | 4553 |
| B | 3340 | 1612 | 8283 | 5594 | – | 2278 | 5255 | 4423 | 3217 | 4839 |
| C | 3794 | 2755 | 9215 | 6326 | – | 2204 | 5279 | 6199 | 3440 | 6001 |
| D | 4555 | 2990 | 8735 | 6560 | – | 2169 | 5692 | 7372 | 6117 | 6633 |
| E | 5960 | 3774 | 9675 | 7153 | – | 2189 | 6215 | 7396 | 7013 | 4725 |
| F | | | | | | | 6501 | 5699 | 7102 | 5454 |
| DMc other | 0.48 | 0.48 | 0.75 | 0.52 | 0.26 | 0.18 | 0.67 | 0.54 | 0.53 | 0.44 |

interception to accommodate for this shift. The estimated shift in this relationship is 0.04, within the range of values for soil pixels. The resulting model explains about 79% of the variation in *LI*. The negative exponential relationship is commonly used to describe attenuation of light within the canopy as function of leaf area index (*LAI*), with normal light extinction coefficients of around 0.65 for *LAI* vs. *LI (or* $LI = 1\text{-}exp^{(-0.65 \times LAI)}$*)*. This also means that *eBeePVI* is linearly related to *LAI* ($LAI = -0.3704 + 9.26 \times eBeePVI$).

### 3.3. Differences between fields within the landscape

There were large differences between fields in the observed yields and the within–plot coefficients of variation at various positions along the catena. In general, fields in the valley yielded more and were less heterogeneous within plots in 2014, but these patterns differed in 2015 (Fig. 3). There was a strong crop type and catena position interaction, evidenced by the large differences in yield and within-plot variability for millet, while differences for sorghum were small. As expected, the within-plot variability was much smaller when satellite images were used, and observed differences between catena positions were not comparable to the UAV.

Relative differences in seasonal mean values of the natural logarithm of ground cover between plots with the same crop type, as derived from the vertical photographs of the quadrats in the plots, were moderately to strongly related to relative differences in yield ($R^2$ values of 0.38–0.71) and vegetative biomass ($R^2$ values of 0.15–0.89, Fig. 4). Relationships were much stronger for millet and sorghum than for maize.

### 3.4. UAV-derived PVI vs. WorldView-derived NDVI

The UAV-derived vegetation indices are strongly related to satellite image-derived *NDVI* (Fig. 5). The *eBeePVI* seemed less sensitive to saturation when compared to satellite *NDVI*, most notably at *NDVI* values above 0.6. The estimates of the spatial coefficients of variation at the plot scale strongly differed between the two image sources. Here, eBee mosaics always feature much higher *CV* values than satellite imagery, as eBee's much smaller instantaneous field of view results in a larger number of contributing values per plot. This higher spatial resolution resolves missing individual plants within rows, and smaller gaps in plant canopies are not visible in WorldView-2 images.

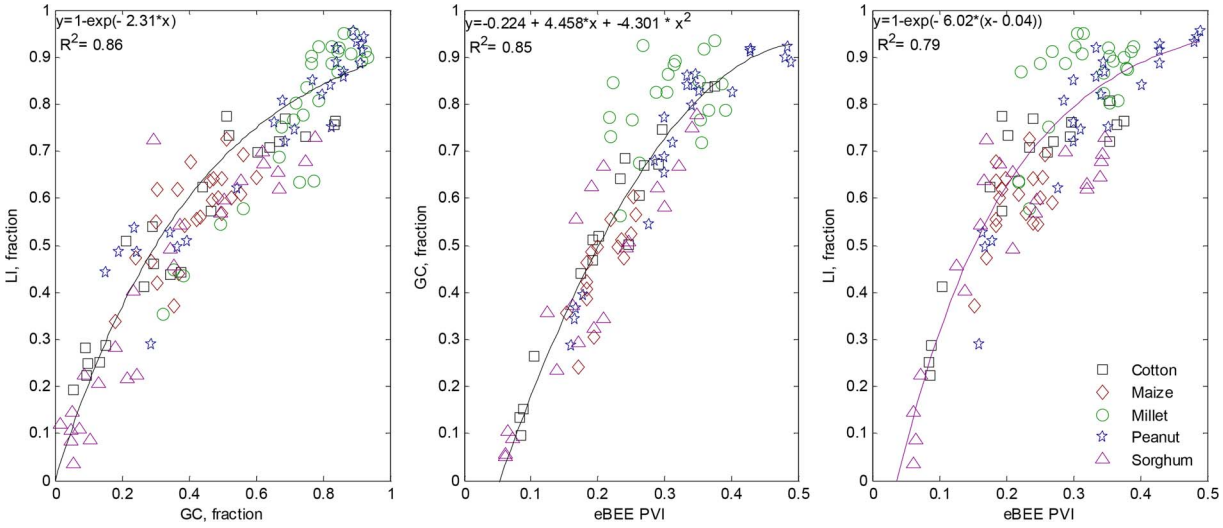


**Fig. 2.** Relationships between ground cover (*GC*), *eBeePVI*, and light interception (*LI*).

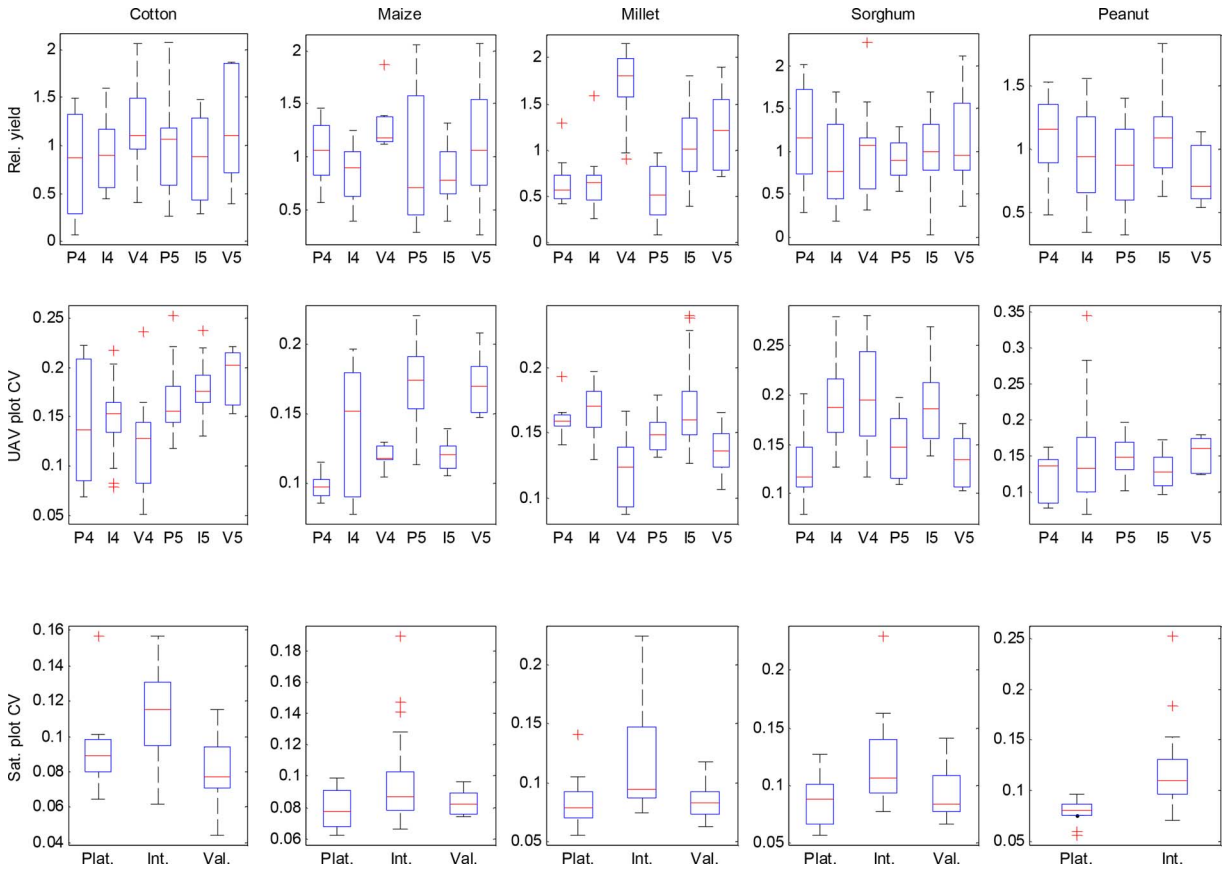


**Fig. 3.** Boxplots showing differences in yields and temporal means of within-plot coefficient of variation (CV) measured with a UAV, (CV of *eBeePVI*) in 2014 (4) and 2015 (5) or with a satellite (CV of *NDVI*, only for 2014) between fields located on the plateau (P), intermediate (I) or valley (V) positions of the landscape. Relative yields were calculated as plot yields divided by the means of all plots with the same crop.

### 3.5. Distributions of vegetation index values within plots

The *eBeePVI*, and therefore also *GC* and *LI*, display a wide range in temporal average *CV* (Fig. 3). For the 2014 WorldView images, all crops except sorghum had smallest *CV* values for valley fields and largest values for fields in intermediate landscape positions. The eBee *CV* values for 2014 followed the same pattern, although maize was, surprisingly, least variable for plateau fields. This was likely due to the late stage in the season with senescent maize crops and the influence of weeds. Coefficients of variation were smaller around the peak of season than in earlier or later growth stages (not shown).

The *eBeePVI* and light interception values were never normally distributed, as reflected in the average skewness of −0.17, −0.18 and −0.31 and kurtosis values of 3.32, 3.28 and 3.49 for plateau,

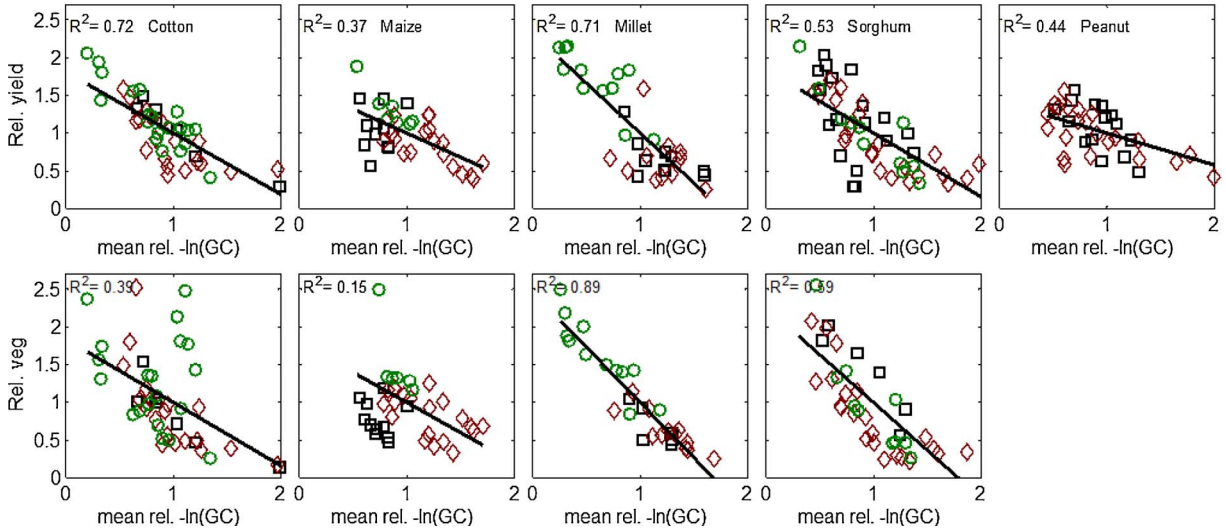


**Fig. 4.** Relationships between the seasonal mean of the natural logarithm of ground coverage (GC) relative to all other plots (times −1), relative yield and vegetative (stover) biomass for the five crop types in 2014. Symbols with green circles, red diamonds and black squares indicate plots in valley, intermediate and plateau fields respectively. (For interpretation of the references to colour in this figure legend, the reader is referred to the web version of this article.)

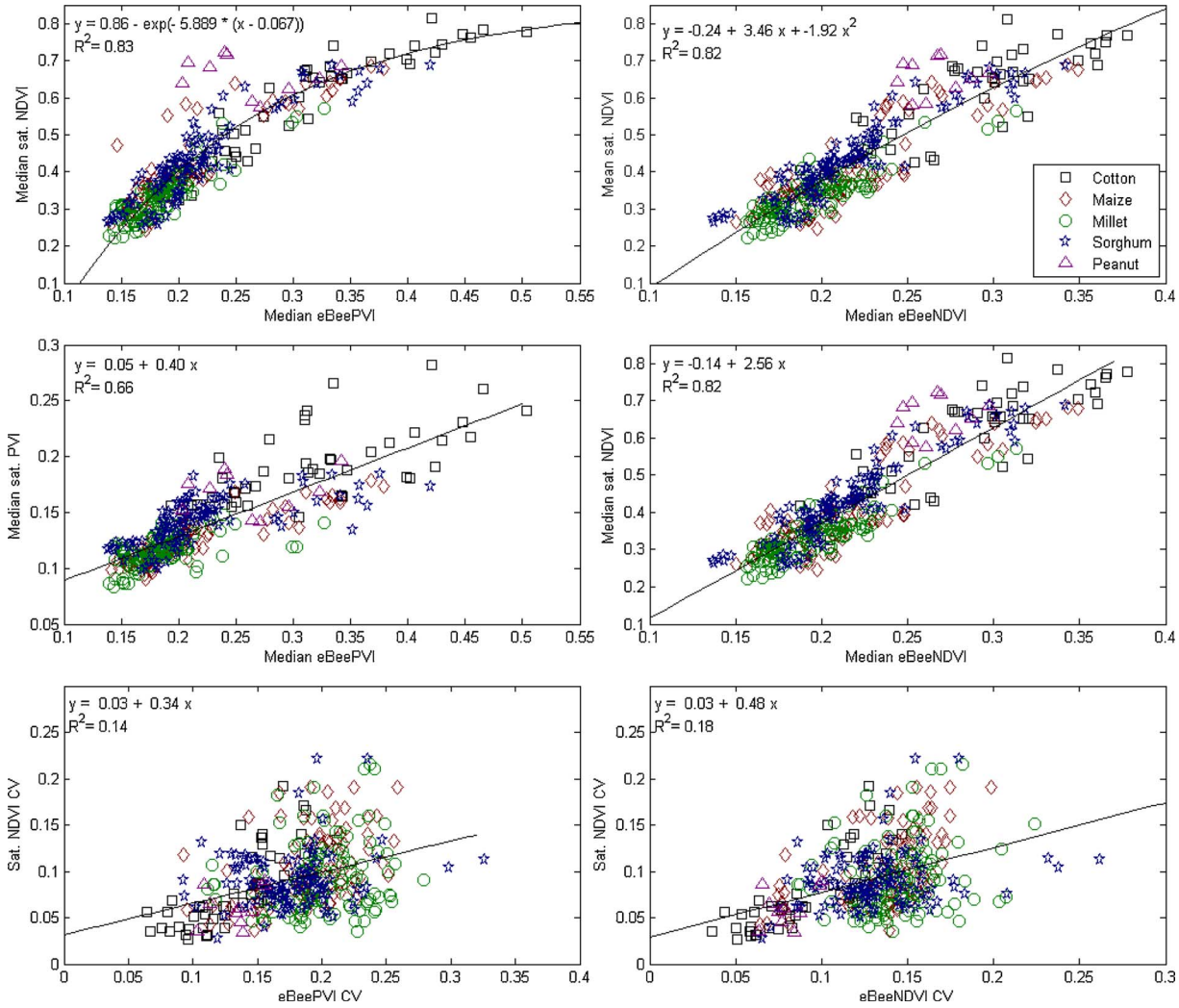


**Fig. 5.** Relationships between spatial coefficients of variation (*CV*, standard deviation/mean) and median *eBeePVI*/*eBeeNDVI* values for plots derived from 2014 UAV mosaics and WorldView-2 satellite images (PVI/NDVI).

intermediate and valley fields respectively. This means that light interception based on the average *eBeePVI* of a plot overestimates the actual light interception, as that relationship saturates at high *eBeePVI* values.

### 3.6. UAV data to assess differences in yield and response

Relative yields are positively correlated with the temporal mean *LI*, but are negatively correlated with the *CV* of *eBeePVI* (Fig. 6). In general, relationships were weakest for maize as crops were already senescing and turning brown in the last part of the 2014 campaign.

### 3.7. Quantification of relative yield and response to fertilizer

The adjusted $R^2$ values for model I ranged between 0.66–0.77 (Table 1). The factor field was by far the most important term in the linear models (Table S2). The fertilizer application in plots and interactions with crops accounted for about 0.14–0.18 of total variation (Model I). The error term included about 0.22 and 0.23 of the total amount of variation in relative yield and relative yield response to fertilizer. Interactions between the factors plot and crop were significant (as expected) indicating that the yield response to fertilizer differed between crop types (Table S2).

Replacing the factor plot reflecting the treatments by ground cover derived from vertical photographs (Model II) explained more of the total variation ($R^2$ of 0.64–0.79, Table 2). This means that the temporal mean of ground coverage also captured some of the within-field, between-plot variation that was not due to the fertilization treatments.

In model III, the plot term was excluded. This model explained most of the variation ($R^2$ of 0.69–0.82, Table 2), as it still explicitly accounted for differences between fields. But when image-derived explanatory variables were included, the plot term was also no longer significant. Image-derived information could therefore explain fertilizer (i.e. plot) effects but also some of the field effect evidenced by the reduced mean squares for the field term when comparing model III with model I (not shown). Temporal means of plot median *eBeePVI* explained more variation than weighted temporal means of light interception (derived from the distributions of *eBeePVI* values) while both terms were significant (Table S2). Also within-plot variation was significant. Significant interactions with the factor crop indicate that *eBeePVI* responses differed between crop types, as expected. The predictions when assessed using the leave-three-plots-out approach, proved robust with $Q^2$ values of 0.75 for relative yield and 0.55 for differences in relative yield within one field (Table 3). These values were slightly better for Model III including eBee image information than for Model II including GC estimates from vertical photographs taken in the field (not shown).

Model IV indicates how well differences between plots located in different fields with the same crop can be assessed. This now includes variation due to management, as fields may vary in seeding time, weed control (etc.), sources of variations that are not explicitly accounted for

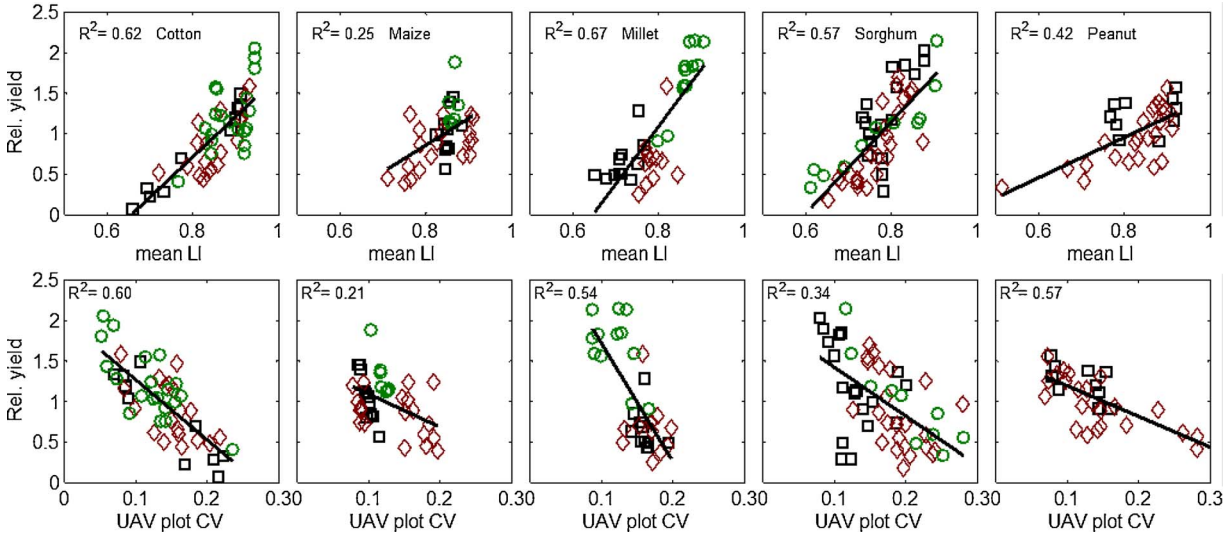


**Fig. 6.** Relationships between relative yields and plot mean light interception and the coefficient of variation (CV) of *eBeePVI* derived from image mosaics for 2014. Symbols with green circles, red diamonds and black squares indicate plots in valley, intermediate and plateau fields respectively. (For interpretation of the references to colour in this figure legend, the reader is referred to the web version of this article.)

**Table 2**
Fraction of variation ($R^2$ adjusted) of relative yield (RY) and the relative yield response (RYR) to the application of fertilizer for models I to VI. Further details can be found in Table S2 of the supplementary materials.

| Model | RY | RYR | RV | RVR |
|---|---|---|---|---|
| I | 0.70 | 0.66 | 0.77 | 0.60 |
| II | 0.78 | 0.77 | 0.79 | 0.64 |
| III | 0.78 | 0.74 | 0.82 | 0.69 |
| IV | 0.45 | 0.48 | 0.46 | 0.59 |
| V | 0.38 | 0.43 | 0.41 | 0.48 |
| VI | 0.41 | 0.47 | 0.51 | 0.48 |

**Table 3**
Cross-validation statistics for linear models, using a leave-one-field-out (LFO) and a leave-three-plots-out (L3O) procedure, for relative vegetative (RV) and generative (RY, yield) plant material, and relative responses (RVR and RYR).

| | LFO | | | | L3O | | | |
|---|---|---|---|---|---|---|---|---|
| | RV | RY | RVR | RYR | RV | RY | RVR | RYR |
| | $R^2$ of linear regression of measured vs. predicted values | | | | | | | |
| Model III | | | | | 0.72 | 0.75 | 0.62 | 0.55 |
| Model IV | 0.21 | 0.22 | 0.39 | 0.52 | 0.41 | 0.40 | 0.45 | 0.55 |
| Model V | 0.24 | 0.25 | 0.33 | 0.41 | 0.36 | 0.39 | 0.40 | 0.45 |
| Model VI | 0.23 | 0.31 | 0.36 | 0.40 | 0.38 | 0.48 | 0.44 | 0.45 |
| | $Q^2$ | | | | | | | |
| Model III | | | | | 0.71 | 0.74 | 0.59 | 0.51 |
| Model IV | 0.11 | 0.13 | 0.39 | 0.51 | 0.41 | 0.40 | 0.45 | 0.55 |
| Model V | 0.22 | 0.22 | 0.31 | 0.40 | 0.36 | 0.38 | 0.40 | 0.45 |
| Model VI | 0.18 | 0.26 | 0.35 | 0.40 | 0.38 | 0.47 | 0.43 | 0.45 |

in the model. Excluding the term field in the model, strongly reduced the total amount of variation that was explained from 0.69-0.82 for model III to 0.45-0.59 for model IV (Table 2). The factors crop light interception and their interactions were significant terms in the model estimating relative yields, but not in the model for estimating differences in relative yield responses to fertilizer (Table S2). Catena position was not included in the model as an explanatory variable, this factor was no longer significant when interactions between the coefficient of variation and light interception with crop were included. Median *eBeePVI* was more important than light interception, reflected by the larger fraction of variation that it accounted for. The coefficient of variation of *eBeePVI* within plots was significant ($p < 0.001$), where a larger *CV* value reduced the RY and RYR to fertilizer, but explained only about 3% of the total variation (Table S2).

The models IV–VI for 2014 proved more robust than for 2015 (Table S3) or for 2014 and 2015 combined with a $Q^2$ value of 0.11–0.52 (Table 3). For example, the relationships fitted with Model IV are reasonably robust when predictions are made for 2014 as the $Q^2$ and $R^2$ values are very similar (Table S3) indicating that no systematic error or bias was encountered. The models predicted relative yields and relative yield responses for fields that were excluded during model calibration reasonably well with $Q^2$ values of 0.38–0.39 for the leave-field-out and 0.47–0.59 for the leave-three-plots-out procedures (Table S3). These values were only slightly better for vegetative material. For 2015 however, these leave-field-out $Q^2$ values were only 0.06–0.36 in the leave-field-out and 0.39–0.43 in the leave-three-out procedures for RY and RYR (Table S3).

Model V reflects how well UAV images can be used to assess differences in yield between fields with the same crop due to differences in light interception and small-scale spatial variability. This model also provides a clear and direct link to crop growth rates, providing more in-depth understanding of underlying processes. The total variation in RY and RYR explained was only 0.38–0.43 (Table 2), indicating that other factors such as drought and pest and disease control had a relatively large influence on the yield differences between fields. The models IV and V for relative yield responses were performing better than the models for relative yield, with higher $Q^2$ values (0.40 vs. 0.22) for the leave-field-out procedure (Table 3).

For most crops, the absolute responses to fertilizer applications were larger for vegetative than for generative material, reflecting low harvest index values (Table S1). However, this did not result in much better predictions for vegetative material, as model accuracy was reasonably comparable between RV and RY and slightly better for RVR than for RYR (Tables 2 and 3).

### 3.8. Influence of seasons and difference DSM

The difference in DSM did not help to further improve as Model VI was not performing much better than Model V when data from 2014 and 2015 was combined (Table 3). The difference *DSM* values did contain some limited amount of additional information for yield only (0.05–0.15, Table S2), but prediction accuracy was poor for 2015 in particular (Table S3).

## 4. Discussion and conclusion

Estimates of light interception derived from UAV mosaics were significantly correlated with crop yield. Although potential plant growth is linearly related to the total amount of light intercepted in the growing season (Monteith, 1972; Monteith, 1977), these relationships cannot be transferred to farmer yields as yield-limiting and–reducing factors also play an important role (van Ittersum et al., 2003; van Ittersum et al., 2013). This analysis shows that these UAV-derived estimates of light interception are indicative of differences in yield between fields of the same crop and within those fields. These estimates also provided means for robust predictions of relative yields and differences in relative yields within fields, although differences between fields were poorly captured. The strong relationships between *eBeePVI* and satellite image-derived *NDVI* allows to scale up relationships from plot to landscape (van der Heijden et al., 2007). The causal relationships between light interception and crop growth rates (Monteith, 1972) provides more confidence than direct correlations between crop yields and vegetation indices, as it also explains why yield differences occur. This was further evidenced by the significant year factor, indicating that relationships differed between 2014 and 2015. Contrastingly, UAV estimates of crop height derived from the difference in digital surface model values between bare soil and vegetated states, provided limited additional information.

The differences in vegetative and generative components of the crop at the end of the season in plots within one field could be assessed with satisfactory accuracy without bias. The accuracy of models decreased when the factor field was excluded in the linear models, indicating that not all biophysical and management factors were captured by vegetation indices, estimates of light interception or within-field variation of those values. Water deficiency and length of the effective growing season (mostly controlled by the sowing date) are two such important factors determining yield. It is therefore not surprising that the explained amounts of variation in these smallholder landscapes were much lower than those reported for intensive farming systems (Li et al., 2016).

The yield response to fertilizer was quantified with reasonable accuracy. This is important as the response to fertilizer, in combination with the price ratio between input and product, is the most important aspect when deciding on the use of inputs in farming systems. For advice on fertilizer investments and amounts to apply, it is commonly assumed that the response to fertilizer is the same for all fields. However, the actual response strongly varies, due to other constraints in *e.g.* non- or poorly responsive fields (Zingore et al., 2007b; Giller et al., 2011; Kurwakumire et al., 2014). In systems with a low application rate, the response to fertilizer is a much more important characteristic than, for example, soil fertility that may not allow to predict the response very well. We envisage a system that uses local reference plots (van Evert et al., 2012) with or without fertilizer to assess the response to applied nutrients at local scale. This has as advantage that a growth response to fertilizer can be assessed mid-season, likely a better indicator of potential response than yield response as later drought, pest and diseases may mask the yield increase potential of fertilizer. This is key information in landscapes with very large differences in soil fertility and yield responses to applied fertilizer within very short distances ($< 250$ m) (Zingore et al., 2007a; Zingore et al., 2008; Tittonell et al., 2013). The growing availability of affordable very-high resolution satellite imagery (Jain et al., 2016), “toy” drone systems, and low-cost methods for non-destructive assessments of local responses to fertilizer using in-field references will help empower extension officers and agronomic experts to better inform farmers.

Large differences in spatial variability between fields located in different catena positions indicate that variability itself is an indicator of soil responsiveness and fertility. Indeed, yields were negatively correlated with spatial variability measured within plots and the coefficient of variation was a significant term in the linear models, for both relative yield and the response to fertilizer. Sub-meter variability will respond to missing plants, and thus indicates poorer growing conditions, partly explaining the reduced response to fertilizer. As also shown here, assessment of spatial variation strongly depends on the spatial resolution of the images. We expect that missing plants or plants with stunted growth strongly affect vegetation index values that are derived from images with spatial resolutions $< 0.5$ m, while in a $4\,m^2$ pixel these differences are averaged out.

Current plant growth models are used to estimate yields at the field scale (van Ittersum et al., 2003; van Ittersum et al., 2013), but implicitly assume homogeneous plant distributions within. Further, crop growth models are calibrated on data from experimental plots. The modeled water-limited yields reflect those conditions, which are generally better than those from farm fields and are, therefore, not the most realistic benchmark to evaluate farmer field performance. Remote sensing estimates of ground cover and light interception are sensitive to canopy gaps associated with missing or stunted plants, as shown by their negatively skewed, non-normal distributions. This indicates that estimates based on only field-means will not represent actual light interception accurately. These estimates can be used as forcing functions, i.e. to provide the light interception as input rather than calculating it, in crop growth models (Qi et al., 2005). Alternatively, they can be used to calibrate model parameters or to filter state variables with observations (Jongschaap, 2006; Dorigo et al., 2007). Further, remotely sensed estimates of initial and maximum radiation interception and phenological development fosters improvement in prediction over conventional modeling techniques (Quiroz et al., 2017). Assimilation of such remotely sensed estimates of crop conditions will help increase the realism and efficiency of modeling approaches in smallholder conditions, enabling benchmarking to water-limited or attainable yields at more detailed spatial scales than previously possible, and allows model simplification (Traoré et al., 2008), and scaling from plot to landscape scales and beyond.

The UAV system used (eBee) carried a simple S110 NIR camera with severe radiometric limitations. Variations in ambient light conditions are major challenges when extracting information from mosaics (Rasmussen et al., 2016). The soil line derived from the RED vs. NIR scatterplots allowed us to construct a robust image time-series. The S110 NIR-derived eBee perpendicular vegetation index was strongly related to ground cover and light interception by crops, providing means to use these systems for meaningful assessments of the crop’s capacity to convert sunlight into biomass (Sinclair and Muchow, 1999). Further estimates of crop height, as derived from the difference in digital surface model values between bare soil and vegetated states, provided limited additional information.

Smallholder fields are spatially variable and, therefore, treatment responses are difficult to interpret (Vanlauwe et al., 2016). The differences in treatment response within one field were captured robustly with simple vertical photographs, but also with UAV estimates of light interception. The sub-meter spatial resolution of UAV imagery allows the capture of within-field variability in crop growth and response, opening possibilities for more accurate management response monitoring. Time-series of UAV or high-resolution satellite imagery can be most useful for hindcasting (Jain et al., 2016), to assess crop growth and yield at local scales (e.g. 10–100 $km^2$) (Burke and Lobell, 2017). Importantly, they will permit more realistic crop growth modeling and yield forecasting in heterogeneous smallholder fields by explicitly incorporating spatial variability of light interception, an omission in most current crop growth models.

## Acknowledgments

This publication was made possible (in part) by the STARS project, an integrated effort to improve our understanding of the use of remote sensing technology in monitoring smallholder farming supported by the Bill and Melinda Gates Foundation (www.stars-project.org). Additional

support was provided by the CGIAR Research Program on Climate Change, Agriculture and Food Security (CCAFS), which is carried out with support from CGIAR Fund Donors and through bilateral funding agreements. For details please visit https://ccafs.cgiar.org/donors. The views expressed in this document cannot be taken to reflect the official opinions of these organisations. The authors would like to acknowledge the field team members: Daouda Sanou (AMEDD), Nema Dembélé (AMEDD), Nouhoum Dembélé (AMEDD), Oumar Diabaté (AMEDD), Gilbert Dembélé (AMEDD), Birama Sissoko (AMEDD), Ousmane Dembélé (AMEDD), Bougouna Sogoba (AMEDD), Issa Kassogué (ICRISAT), Ousmane Ndiaye (ICRISAT), Fatoumata Sagounta (ICRISAT), Adja R. Sangaré (ICRISAT) and students Wilmar van Ommeren, Cass Gooskens, Bastiaen Boekelo, Joel Davidse, Frederic de Schaetzen and Guillaume Chomé for their contributions.

## Appendix A. Supplementary data

Supplementary data associated with this article can be found, in the online version, at https://doi.org/10.1016/j.fcr.2018.02.018.

## References

Bendig, J., Bolten, A., Bennertz, S., Broscheit, J., Eichfuss, S., Bareth, G., 2014. Estimating biomass of barley using crop surface models (CSMs) derived from UAV-based RGB imaging. Remote Sens. 6, 10395–10412.

Blaes, X., Traore, P.C.S., Schut, A.G.T., Ajeigbe, H.A., Chome, G., Boekelo, B., Diancoumba, M., Goita, K., Inuwa, A.H., Zurita-Milla, R., Stratoulias, D., 2015. STARS-ISABELA Field Data Collection Protocols. Internal Document. Spurring a Transformation for Agriculture Through Remote Sensing (STARS). West Africa Work Package on 'Imagery for Smallholders–Activating Business Entry Points and Leveraging Agriculture' (ISABELA). Version 10c. Nov. 2015. Universite Catholique de Louvain. International Crops Research Institute for the Semi-Arid Tropics, pp. 42.

Blaes, X., Chomé, G., Lambert, M.-J., Traore, P.C.S., Schut, A.G.T., Defoury, P., 2016. Quantifying fertilizer application response variability with VHR satellite time-series in a rainfed smallholder cropping system of Mali. Remote Sens. 8, rs8060531.

Bouman, B.A.M., Goudriaan, J., 1989. Estimation of crop growth from optical and microwave soil cover. Int. J. Remote Sens. 10, 1843–1855.

Burke, M., Lobell, D.B., 2017. Satellite-based assessment of yield variation and its determinants in smallholder African systems. Proc. Natl. Acad. Sci. U. S. A. 114, 2189–2194.

Dorigo, W.A., Zurita-Milla, R., de Wit, A.J.W., Brazile, J., Singh, R., Schaepman, M.E., 2007. A review on reflective remote sensing and data assimilation techniques for enhanced agroecosystem modeling. Int. J. Appl. Earth Obs. Geoinf. 9, 165–193.

Giller, K.E., Tittonell, P., Rufino, M.C., van Wijk, M.T., Zingore, S., Mapfumo, P., Adjei-Nsiah, S., Herrero, M., Chikowo, R., Corbeels, M., Rowe, E.C., Baijukya, F., Mwijage, A., Smith, J., Yeboah, E., van der Burg, W.J., Sanogo, O.M., Misiko, M., de Ridder, N., Karanja, S., Kaizzi, C., K'Ungu, J., Mwale, M., Nwaga, D., Pacini, C., Vanlauwe, B., 2011. Communicating complexity: integrated assessment of trade-offs concerning soil fertility management within African farming systems to support innovation and development. Agric. Syst. 104, 191–203.

Goudriaan, J., Van Laar, H.H., 1994. Modelling Potential Crop Growth Processes: Textbook with Exercises. Kluwer Academic Publishers Dordrecht, The Netherlands.

Jain, M., Srivastava, A., Balwinder-Singh Joon, R., McDonald, A., Royal, K., Lisaius, M., Lobell, D., 2016. Mapping smallholder wheat yields and sowing dates using micro-satellite data. Remote Sens. 8, 860.

Jongschaap, R.E.E., 2006. Run-time calibration of simulation models by integrating remote sensing estimates of leaf area index and canopy nitrogen. Eur. J. Agron 24, 316–324.

Khot, L.R., Sankaran, S., Carter, A.H., Johnson, D.A., Cummings, T.F., 2016. UAS imaging-based decision tools for arid winter wheat and irrigated potato production management. Int. J. Remote Sens. 37, 125–137.

Kurwakumire, N., Chikowo, R., Mtambanengwe, F., Mapfumo, P., Snapp, S., Johnston, A., Zingore, S., 2014. Maize Productivity and Nutrient and Water Use Efficiencies Across Soil Fertility Domains on Smallholder Farms in Zimbabwe 164. pp. 136–147.

Li, W., Niu, Z., Chen, H., Li, D., Wu, M., Zhao, W., 2016. Remote estimation of canopy height and aboveground biomass of maize using high-resolution stereo images from a low-cost unmanned aerial vehicle system. Ecol. Indic. 67, 637–648.

Monteith, J.L., 1972. Solar-radiation and productivity in tropical ecosystems. J. Appl. Ecol. 9, 747–766.

Monteith, J.L., 1977. Climate and efficiency of crop production in Britain: philos. Trans. R. Soc. Lond. Ser. B-Biol. Sci. 281, 277–294.

PIRT-Projet Inventaire des Ressources Terrestres, 1983. Les ressources terrestres au Mali. Government of Mali/USAID/TAMS, New York.

Qi, A., Kenter, C., Hoffmann, C., Jaggard, K.W., 2005. The Broom's Barn sugar beet growth model and its adaptation to soils with varied available water content. Eur. J. Agron 23, 108–122.

Quiroz, R., Loayza, H., Barreda, C., Gavilán, C., Posadas, A., Ramírez, D.A., 2017. Linking process-based potato models with light reflectance data: does model complexity enhance yield prediction accuracy? Eur. J. Agron 82, 104–112.

Rasmussen, J., Ntakos, G., Nielsen, J., Svensgaard, J., Poulsen, R.N., Christensen, S., 2016. Are vegetation indices derived from consumer-grade cameras mounted on UAVs sufficiently reliable for assessing experimental plots? Eur. J. Agron. 74, 75–92.

Rondeaux, G., Steven, M., Baret, F., 1996. Optimization of soil-adjusted vegetation indices. Remote Sens. Environ. 55, 95–107.

Sankaran, S., Khot, L.R., Espinoza, C.Z., Jarolmasjed, S., Sathuvalli, V.R., Vandemark, G.J., Miklas, P.N., Carter, A.H., Pumphrey, M.O., Knowles, N.R.N., Pavek, M.J., 2015. Low-altitude, high-resolution aerial imaging systems for row and field crop phenotyping. A review. Eur. J. Agron 70, 112–123.

Schut, A.G.T., Gherardi, S.G., Wood, D.A., 2010. Empirical models to quantify the nutritive characteristics of annual pastures in south-west Western Australia. Crop Pasture Sci. 61, 32–43.

Sinclair, T.R., Muchow, R.C., 1999. Radiation use efficiency. Adv. Agron 215–265.

Stratoulias, D., De By, R.A., Zurita-Milla, R., Bijker, W., Tolpekin, V., Schulthess, U., Ahmed, Z.U., 2015. The potential of very high spatial resolution remote sensing in applications in smallholder agriculture. ACRS 2015-36th Asian Conference on Remote Sensing: Fostering Resilient Growth in Asia, Proceedings.

Tittonell, P., Giller, K.E., 2013. When yield gaps are poverty traps: the paradigm of ecological intensification in African smallholder agriculture. Field Crops Res. 143, 76–90.

Tittonell, P., Vanlauwe, B., Leffelaar, P.A., Rowe, E.C., Giller, K.E., 2005a. Exploring diversity in soil fertility management of smallholder farms in western Kenya: i. Heterogeneity at region and farm scale. Agric. Ecosyst. Environ. 110, 149–165.

Tittonell, P., Vanlauwe, B., Leffelaar, P.A., Shepherd, K.D., Giller, K.E., 2005b. Exploring diversity in soil fertility management of smallholder farms in western Kenya: II. Within-farm variability in resource allocation, nutrient flows and soil fertility status. Agric. Ecosyst. Environ. 110, 166–184.

Tittonell, P.A., Vanlauwe, B., Corbeels, M., Giller, K.E., 2008. Yield gaps, nutrient use efficiencies and response to fertilisers by maize across heterogeneous smallholder farms of western Kenya. Plant Soil 313, 19–37.

Tittonell, P., Muriuki, A., Klapwijk, C.J., Shepherd, K.D., Coe, R., Vanlauwe, B., 2013. Soil heterogeneity and soil fertility gradients in smallholder farms of the east African highlands. Soil Sci. Soc. Am. J. 77, 525–538.

Traoré, P.C.S., Bostick, W.M., Jones, J.W., Koo, J., Goïta, K., Bado, B.V., 2008. A simple soil organic-matter model for biomass data assimilation in community-level carbon contracts. Ecol. Appl. 18, 624–636.

Traore, B., Corbeels, M., van Wijk, M.T., Rufino, M.C., Giller, K.E., 2013. Effects of climate variability and climate change on crop production in southern Mali. Eur. J. Agron. 49, 115–125.

Vanlauwe, B., Coe, R., Giller, K.E., 2016. Beyond averages: new approaches to understand heterogeneity and risk of technology success or failure in smallholder farming. Exp. Agric. 1–23. http://dx.doi.org/10.1017/S0014479716000193.

van Evert, F.K., Booij, R., Jukema, J.N., ten Berge, H.F.M., Uenk, D., Meurs, E.J.J.B., van Geel, W.C.A., Wijnholds, K.H., Slabbekoorn, J.J.H., 2012. Using crop reflectance to determine sidedress N rate in potato saves N and maintains yield. Eur. J. Agron 43, 58–67.

van Ittersum, M.K., Leffelaar, P.A., Van Keulen, H., Kropff, M.J., Bastiaans, L., Goudriaan, J., 2003. On approaches and applications of the Wageningen crop models. Eur. J. Agron 18, 201–234.

van Ittersum, M.K., Cassman, K.G., Grassini, P., Wolf, J., Tittonell, P., Hochman, Z., 2013. Yield gap analysis with local to global relevance-a review. Field Crops Res. 143, 4–17.

van Ittersum, M.K., van Bussel, L.G.J., Wolf, J., Grassini, P., van Wart, J., Guilpart, N., Claessens, L., de Groot, H., Wiebe, K., Mason-D'Croz, D., Yang, H., Boogaard, H., van Oort, P.A.J., van Loon, M.P., Saito, K., Adimo, O., Adjei-Nsiah, S., Agali, A., Bala, A., Chikowo, R., Kaizzi, K., Kouressy, M., Makoi, J.H.J.R., Ouattara, K., Tesfaye, K., Cassman, K.G., 2016. Can sub-Saharan Africa feed itself? Proc. Natl. Acad. Sci. 113, 14964–14969.

van der Heijden, G.W.A.M., Clevers, J.G.P.W., Schut, A.G.T., 2007. Combining close-range and remote sensing for local assessment of bio-physical characteristics of arable land. Int. J. Remote Sens. 28, 5485–5502.

Xu, D., Guo, X., 2013. A study of soil line simulation from landsat images in mixed grassland. Remote Sens. 5, 4533–4550.

Zhang, C., Kovacs, J.M., 2012. The application of small unmanned aerial systems for precision agriculture: a review. Precis. Agric. 13, 693–712.

Zingore, S., Murwira, H.K., Delve, R.J., Giller, K.E., 2007a. Influence of nutrient management strategies on variability of soil fertility, crop yields and nutrient balances on smallholder farms in Zimbabwe. Agric. Ecosys. Environ. 119, 112–126.

Zingore, S., Murwira, H.K., Delve, R.J., Giller, K.E., 2007b. Soil type: management history and current resource allocation: three dimensions regulating variability in crop productivity on African smallholder farms. Field Crops Res. 101, 296–305.

Zingore, S., Delve, R.J., Nyamangara, J., Giller, K.E., 2008. Multiple benefits of manure: the key to maintenance of soil fertility and restoration of depleted sandy soils on African smallholder farms. Nutr. Cycl. Agroecosyst. 80, 267–282.

Zingore, S., Tittonell, P., Corbeels, M., van Wijk, M.T., Giller, K.E., 2011. Managing soil fertility diversity to enhance resource use efficiencies in smallholder farming systems: a case from Murewa District, Zimbabwe. Nutr. Cycl. Agroecosyst. 90, 87–103.